Carbohydrate Polymer Technologies and Applications 4 (2022) 100257

Contents lists available at ScienceDirect

Carbohydrate Polymer Technologies and Applications

journal homepage: www.sciencedirect.com/journal/carbohydrate-polymer-technologies-and-applications

Chitosan-based Maillard self-reaction products: Formation, characterization, antioxidant and antimicrobial potential

Aliaksandr Kraskouski [a,*], Kseniya Hileuskaya [a], Viktoryia Nikalaichuk [a], Alena Ladutska [b], Volha Kabanava [a,c], Wanzi Yao [d], Lijun You [d]

[a] Institute of Chemistry of New Materials of National Academy of Sciences of Belarus, 220141, 36 Skaryna str., Minsk, Belarus
[b] Institute of Microbiology of National Academy of Sciences of Belarus, 220141, 2 Kuprevich str., Minsk, Belarus
[c] Belarusian State University, 220030, 4 Nezavisimosti Ave., Minsk, Belarus
[d] School of Food Science and Engineering, South China University of Technology, Guangzhou, Guangdong 510640, China

ARTICLE INFO

Keywords:
Chitosan
Maillard reaction
Melanoidins
Antioxidant activity
Antimicrobial activity

ABSTRACT

In this work, new chitosan derivatives (CS1-CS6) were obtained by short-term hydrothermal treatment. The formation of chitosan derivatives occurred through two simultaneous processes: hydrolysis and Maillard self-reaction. The synthesized chitosan-based Maillard self-reaction products were characterized by physical measurements and spectroscopic methods (viscometry, UV–Vis, FTIR, ^{1}H NMR, TGA and XRD). The results showed that hydrothermal treatment of chitosan solutions leads to a significant decrease (from ~ 66500 up to ~ 20150 Da) in the viscosity-average molecular weight of polymer. It has been shown that the antiradical activity of CS1-CS6 was 2-5 times higher in comparison with the activity of unmodified chitosan (1.42 μg ascorbic acid equivalents/mg). The enhanced (R value ≥ 4-5) antimicrobial activity of CS1-CS5 derivatives against gram-negative and gram-positive bacteria including thermophilic highly heat-resistant *Geobacillus stearothermophilus* has been demonstrated.

1. Introduction

Currently, artificial preservatives are widely used to ensure microbial food safety, as well as its nutritional value and organoleptic characteristics. At the same time, the search for natural antimicrobials is relevant due to consumers' concern on health issues. Moreover, the widespread use of conventional antibiotics is leading to the emergence of multidrug-resistant bacteria, reinforcing the research focus on the natural antimicrobial agents in the food industry (Quinto et al., 2019).

Chitosan is actively used in medicine (Bakshi et al., 2020; Muzzarelli et al., 2014; Verlee et al., 2017) due to its unique physicochemical, biological, ecological and physiological properties: non-toxicity, biocompatibility, biodegradability, stability in the natural environment, antibacterial activity etc. However, there are some drawbacks limiting the use of chitosan: low solubility in water and physiological media and, as a result, insufficient bioavailability, weak antioxidant activity, complicated methods for obtaining polysaccharide derivatives. In general, the antioxidant activity of chitosan is significantly inferior to classical antioxidants, which also limits its use as a substrate for the creation of pharmaceuticals and dietary supplements (Yang et al., 2020). Chemical modification of chitosan, including by conjugation with molecules of biologically active substances (oxycinnamic acids, proteins, etc.), makes it possible to obtain polymer derivatives with improved characteristics (Varlamov et al., 2020). Thus, the introduction of additional functional groups into chitosan leads to enhance its antiviral and antibacterial activity, increase its immunostimulatory, adjuvant, adaptogenic, antihypoxic, radioprotective and hemostatic effects (Bakshi et al., 2020; Muzzarelli et al., 2014; Verlee et al., 2017), as well as improve its antioxidant (Alexandrova et al., 2016) and mucoadhesive (Ways et al., 2018) properties. The conjugation of chitosan is most often carried out by the standard carbodiimide method (Nikalaichuk et al., 2022), the drawback of which is the high cost of reagents for carbodiimide activation of functional groups. At the same time, carbonyl-amine interactions can occur under the influence of temperature, for example, when amino acids are heated with sugars, i.e. melanoidin formation or the Maillard reaction (MR). The amino groups of chitosan can react with the carbonyl group of sugar to form of Maillard reaction products (MRPs) (Chang et al., 2011; Kanatt et al., 2008; Rao et al., 2011).

* Corresponding author.
E-mail address: aleks.kraskovsky@gmail.com (A. Kraskouski).

https://doi.org/10.1016/j.carpta.2022.100257

Available online 7 November 2022

In recent years, a lot of data on the physiological and biochemical significance of melanoidins have been obtained. It has been established that the MRPs have a higher biological activity compared to the initial components (Gullón et al., 2016; Tran et al., 2019; Yang et al., 2020). The main condition for the Maillard reaction to proceed is prolonged heating at high temperature. Thus, the improved antiradical activity of chitosan derivatives obtained after keeping the polymer in the presence of fructose at 80°C for 8 h has been shown (Yang et al., 2020). A significant reduction in the reaction time can be achieved by hydrothermal treatment of the reaction mixtures and/or an increase in the concentration of sugar. Thus, the authors (Tran et al., 2019) not only reduced the reaction time by 4 times due to hydrothermal conditions, but also obtained products with improved solubility and antidiabetic potential. Chitosan-based melanoidins are promising material for the food industry and medicine. It has been shown that chitosan and galactose derivatives, when added to apple juice, improve its quality, exhibit high antiamylase and antiglucosidase activity, while for chitosan and nisin derivatives *in vivo*, the effect of preventing obesity and intestinal dysbacteriosis was noted (Yang et al., 2020).

As mentioned above, the presence of free amino groups in chitosan allows it to be as amino group donor in the Maillard reaction. On the other hand, chitosan also contains reducing fragments, for example, hemiacetal hydroxyl groups, so oligochitosan (hydrolyzed form of chitosan) can act as a carbonyl group donor (Jung et al., 2014; Sun et al., 2018). Thus, it is possible to form MRPs between the free amino groups of chitosan and carbonyl groups of its hydrolyzed form (oligomer) upon heating. However, no sufficient information is available with regard to MRPs from chitosan alone.

In this study, we hypothesized that modification of chitosan by Maillard self-reaction without any additives via hydrothermal treatment would enhance the antioxidant and antimicrobial activities of polysaccharide. For this purpose, the hydrothermal synthesis and characterization of chitosan-based MRPs was reported. In addition, the antioxidant and antimicrobial activities of the obtained MRPs were evaluated.

2. Materials and methods

2.1. Materials

Low molecular weight chitosan (CS, M_w 30 kDa, degree of deacetylation > 90%) was purchased from Glentham Life Sciences (UK). 2,2′-Azino-bis(3-ethylbenzothiazoline-6-sulfonic acid)diammonium salt (ABTS, ~ 98%) was obtained from Sigma-Aldrich (Germany). Folin-Ciocalteu reagent was purchased from Merck KGaA (Germany). The other used reagents from commercial sources were analytical grade and employed without future purification.

2.2. Preparation of Maillard self-reaction products (MSRPs)

Chitosan solutions (3.4, 10, 17, 23.8, 34, 68 mg/mL) were prepared by dissolving in 2% v/v glacial acetic acid solution and stirred for 16 h at 700 rpm (RH Basic 2, IKA, Germany) at 20-22°C. Next, the solutions were autoclaved (GK-100-3, JSC TZMOI, Russia) for 1 h (121°C, 1.5 bars). After heating, the samples were cooled and stored in the dark at 4 ±1°C for further analyses. Hereinafter in text, the samples were named as CS1, CS2, CS3, CS4, CS5, and CS6 respectively.

2.3. Characterization

2.3.1. Measurement of browning

The browning of the obtained samples was determined by UV-Vis spectroscopy. The UV-Vis absorption spectra were recorded in the 220-600 nm range using the spectrofluorimeter CM2203 (Solar, Belarus). For absorbance measurements at 282-289 nm, the samples were diluted 20 times using distilled water, while at 420 nm – 2 times, except for CS6 (3-fold dilution). To calculate A_{max}/A_{420} ratio the samples were diluted to chitosan concentration of 0.9 mg/mL, and the absorption intensity at 282-289 (A_{max}) and 420 (A_{420}) nm was measured.

2.3.2. Measurement of fluorescence

Suitable dilutions of the samples were taken for measurement of fluorescence as described by authors (Li et al., 2019; Morales & Jiménez-Pérez, 2001) using the spectrofluorimeter CM2203 (Solar, Belarus). Measurement of fluorescence was carried out for the samples diluted 100 times using distilled water. The fluorescence intensity was measured at an excitation wavelength of 340 nm and emission wavelength of 425 nm.

2.3.3. Fourier transform infrared (FTIR) spectroscopy

FTIR spectra of chitosan and chitosan derivatives were recorded using Tensor-27 spectrometer (Bruker, Germany), operating in the attenuated total reflection (ATR) mode, by scanning along spectrum range from 4000 to 400 cm^{-1}. Data collection was performed with a 4 cm^{-1} spectral resolution and 32 scans.

2.3.4. Nuclear magnetic resonance (NMR) spectroscopy

^1H NMR analysis was performed by Bruker Avance 500 MHz high-resolution NMR spectrometer (Bruker, USA). Samples were dissolved in D_2O to give a concentration of 15 mg/mL. The chitosan acetate was used as a standard.

2.3.5. Thermogravimetric analysis (TGA)

A thermogravimetric analysis (TGA) was carried out to determine the thermal stability of the CS and CS1-CS6 samples using TGA instrument STA 449 F3 (Netzsch, Germany) under the following conditions: crucible Al_2O_3, temperature range from 25 to 600°C, heating rate – 5K/min, oxygen/nitrogen atmosphere, weight of samples 11-19 mg.

2.3.6. X-ray diffraction analysis (XRD)

X-ray diffraction analysis was carried out on a D8 ADVANCE ECO diffractometer (Bruker, Germany) using CuKα radiation (λ = 1.5406 Å) at 2θ = 10-60° with a step size of 0.0133°.

2.3.7. Determination of the viscosity-average molecular weight

The viscosity-average molecular weight of neat and modified chitosans was determined from the flow rate of their solutions (0.090-0.722 gram/deciliter) in 2% CH_3COOH/0.2 M CH_3COONa buffer in the capillary. The intrinsic viscosity of a polymer solution is related to the polymer molecular weight according to the Mark-Houwink-Sakurada equation (Kasaai, 2007).

$$[\eta] = K \cdot M_v^{\alpha} \quad (1)$$

where [η] is the intrinsic viscosity, M_v - the viscosity-average molecular weight, K and α are the constants for a given solute-solvent system (2% CH_3COOH/0.2 M CH_3COONa, $K=1{,}38 \cdot 10^{-4}$ deciliter/gram, α=0,85).

The viscometric parameters were measured by VPZh-2 capillary viscometer (capillary diameter was 0.56 mm) at 25.0±0.1°C using Thermo Haake DC30 temperature-controlled bath. The experimental determination of the intrinsic viscosity was started with the detection of the flow times of the solvent (t_o) and the sample solutions of different concentrations (0.090-0.722 gram/deciliter). The flow time values were averaged for at least five measurements. For each sample concentration, the reduced viscosity and inherent viscosity were calculated by Eqs. (2)–(5), and then were plotted against concentration (C). Double extrapolation of plots of reduced viscosity and inherent viscosity to zero concentration was performed. The value of intrinsic viscosity was determined by calculation the average of the two intercept values.

$$\text{relative viscosity, } \eta_{rel} = t_{average} / t_0 \quad (2)$$

$$\text{specific viscosity, } \eta_{sp} = \eta_{rel} - 1 \quad (3)$$

$$\text{reduced viscosity, } \eta_{red} = \eta_{sp}/\mathrm{C} \quad (4)$$

$$\text{inherent viscosity, } \eta_{inh} = \ln\eta_{rel}C \quad (5)$$

2.3.8. Antioxidant assays

$ABTS^+$ radical-scavenging activity. The ABTS radical scavenging activity was evaluated according to the method described by Re et al. (1999). The $ABTS^+$ radical was generated by mixing 7 mM ABTS solution, containing 2.45 mM potassium persulfate, in the dark overnight (more than 16 h) at 20-22°C. The $ABTS^{\bullet+}$ stock solution was diluted with 2% CH_3COOH/0.2 M CH_3COONa buffer to obtain an absorbance of 0.70 ±0.03 units at 734 nm. The working $ABTS^{\bullet+}$ solution (1 mL) was mixed with 100 μL of the sample diluted to chitosan concentration of 3.1 mg/mL, and the absorbance was measured at 734 nm using the spectrofluorimeter CM2203 (Solar, Belarus) after 6 min of incubation at 20-22°C. The $ABTS^{\bullet+}$ solution without sample was used as a control. The scavenging effect was calculated according to the following equation:

$$\text{Scavenging effect } (\%) = \left(A_{control} - A_{sample}\right)/A_{control} \cdot 100 \quad (6)$$

where $A_{control}$ and A_{sample} is the absorption intensity at 734 nm of control and sample respectively.

$ABTS^+$ radical-scavenging activity of the samples was expressed as μg of ascorbic acid equivalents (AE)/mg of the sample by comparing the percent scavenging activity with that of ascorbic acid. A calibration curve was prepared with different concentrations of ascorbic acid (5–200 μM). The equation obtained for ascorbic acid standard curve was $y = 0.4029x - 0.0006$ and the R^2 value was 0.9995.

Reducing power. The reducing power of CS and CS1-CS6 samples was quantified by the following method. Briefly, 3.1 mg/mL of each sample was added in a universal bottle followed by 1.25 mL of diluted 10 times Folin-Ciocalteu reagent. The content of the bottle was mixed thoroughly. After 3 min, 1 mL of sodium carbonate (7.5 wt.%) was added and the mixture was allowed to stand for 1 h at 20-22°C. The absorbance was measured at 765 nm in a spectrophotometer. The same procedure was repeated for all standard ascorbic acid solutions at different concentrations (0.0025, 0.0125, 0.025, 0.05, 0.1, 0.25, 0.5, 1 mM). The equation obtained for ascorbic acid standard curve was $y = 0.9017x - 0.0116$ and the R^2 value was 0.9979. The reducing power of the samples was determined as μg of ascorbic acid equivalent, using an equation. Data presented were averaged for duplicate measurements.

2.3.9. Antibacterial activity

The test cultures were bacterial strains *Bacillus* sp. BIM B-210, *Escherichia coli* BIM B-378, *Pseudomonas aeruginosa* BIM B-153, *Staphylococcus* sp. BIM B-798G, *Geobacillus stearothermophilus* BIM B-140 from the Belarusian collection of non-pathogenic microorganisms. The bacteria *Bacillus* sp. BIM B-210, *E. coli* BIM B-378, *P. aeruginosa* BIM B-153, *Staphylococcus* sp. BIM B-798G were grown in nutrient broth (NB) (Condalab, Spain) at 37±1°C for 24 h, while *G. stearothermophilus* BIM B-140 - at 50±1°C for 24 h. CS and CS1-CS5 samples were inoculated with test cultures of microorganisms at cell concentration 1.0×10^9 CFU/mL (4.5 mL of the sample and 0.5 mL of liquid bacterial culture). Upon 24 h incubation a series of tenfold dilution was prepared from CS and CS1-CS5 samples seeded with bacterial culture to count viable bacterial cells (CFU/mL). All experiments were carried out in triplicate.

2.4. Statistical analysis

The obtained results were presented as mean ± standard deviation. The statistical analysis of the data was performed using the one-way analysis of variance (ANOVA) with a significant level of $p = 0.05$. The value of $p < 0.05$ was considered to be statistically significant.

3. Results and discussion

3.1. Measurement of browning and fluorescence of chitosan MSRPs

The stock solutions of chitosan were transparent and colorless, only solutions of chitosans with high concentration (23.8, 34 and 68 mg/mL) were colored in a weak lemon. After hydrothermal treatment the reaction mixtures remained transparent, but had different browning intensity (BI) (Fig. S1).

The Fig. 1a depicts the UV-vis absorbance spectra at 220÷600 nm of all CS solution samples after hydrothermal treatment (CS concentration was 0.9 mg/mL). The intense peak at 282 nm in the absorption spectra of the reaction mixtures in comparison with the spectrum of the neat chitosan was observed. With an increase in the concentration of chitosan solution a bathochromic shift (up to 289 nm) of the absorption maximum at 282 nm occured, while the peak became asymmetric (Fig. 1a). Moreover, a hyperchromic effect in the UV-vis spectra of CS1-CS6 samples was also observed: the absorption intensity at 282-289 and 420 nm increased (Fig. 1b). Absorption at 282-289 nm was due to carbonyl in the aldehyde and ketone groups. The asymmetry of the absorption band was caused by the appearance of a shoulder at 325 nm, which may be due to the electronic transition n→π* in C=O and N=O bonds (Li et al., 2019) and the formation of the light-emitting structure. During hydrothermal treatment of chitosan solutions in acetic acid the hydrolysis reaction with the elimination of aminoglucosopyranose and acetylaminoglucopyranose fragments with reducing aldehyde groups (Fig. 2, I stage) can occur, which react with amino groups of the main chitosan chain (Fig. 2, II stage). As mentioned above, the interaction of reducing sugars with carbohydrates at high temperatures is attributed to the Maillard reaction (Affes et al., 2021; Liu et al., 2020). In the intermediate stages both compounds with high absorptive capacity in UV and colored ones are formed. At the same time, absorption at 420 nm is characteristic only for the final brown products of the condensation reaction of carbohydrates and sugars – melanoidins (Hafsa et al., 2021; Tran et al., 2019). Thus, the hyperchromic effect in the absorption spectra of CS1-CS6 samples was caused by the increase in amount of MSRPs (intermediates and brown products) with the increase in the concentration of chitosan. The extent of the Maillard reaction is characterized by the ratio of absorption at 282-289 nm (A_{max}) to 420 nm. The decrease of A_{max}/A_{420} indicated that the reaction was in the final stage (Gullón et al., 2016; Tran et al., 2019). The conversion of chitosan to MPs is shown in Fig. 1b. It was found that with the increase in the concentration of chitosan tenfold, the conversion increases by ~ 80%. Thus, the lowest value of A_{max}/A_{420} ratio was established for CS5 and CS6 samples (7.8 and 6.1, respectively), indicating the formation of brown products from the intermediates.

Intermediates of the Maillard reaction have UV absorption and fluorescence (Gullón et al., 2016), as well as strong reducing power (Hafsa et al., 2019). Therefore, to assess the conversion and formation of MSRPs with antiradical activity, it is more efficient to study the fluorescence of reaction systems in comparison with UV investigation (Morales & Jiménez-Pérez, 2001). The color change of the reaction mixture (the so-called browning) occurs only after reaching the maximum fluorescence intensity (i.e. formation of intermediates), which indicates that fluorogens are the precursors of brown pigments (melanoidins) (Gullón et al., 2016; Matiacevich et al., 2005). At the same time, it is known that chitosan derivatives with better solubility, antioxidant and antimicrobial capacity are formed when the MR is more advanced (Hafsa et al., 2021; Kaewtathip et al., 2022; Kosaraju et al., 2010; Nooshkam et al., 2019). The Fig. 3 shows the fluorescence intensity of the reaction mixtures of CS1-CS6. It has been established, that hydrothermal treatment of chitosan solution leads to increase in its fluorescence intensity due to the formation of fluorescent MSRPs. As expected, the amount of fluorescent products of the Maillard reaction

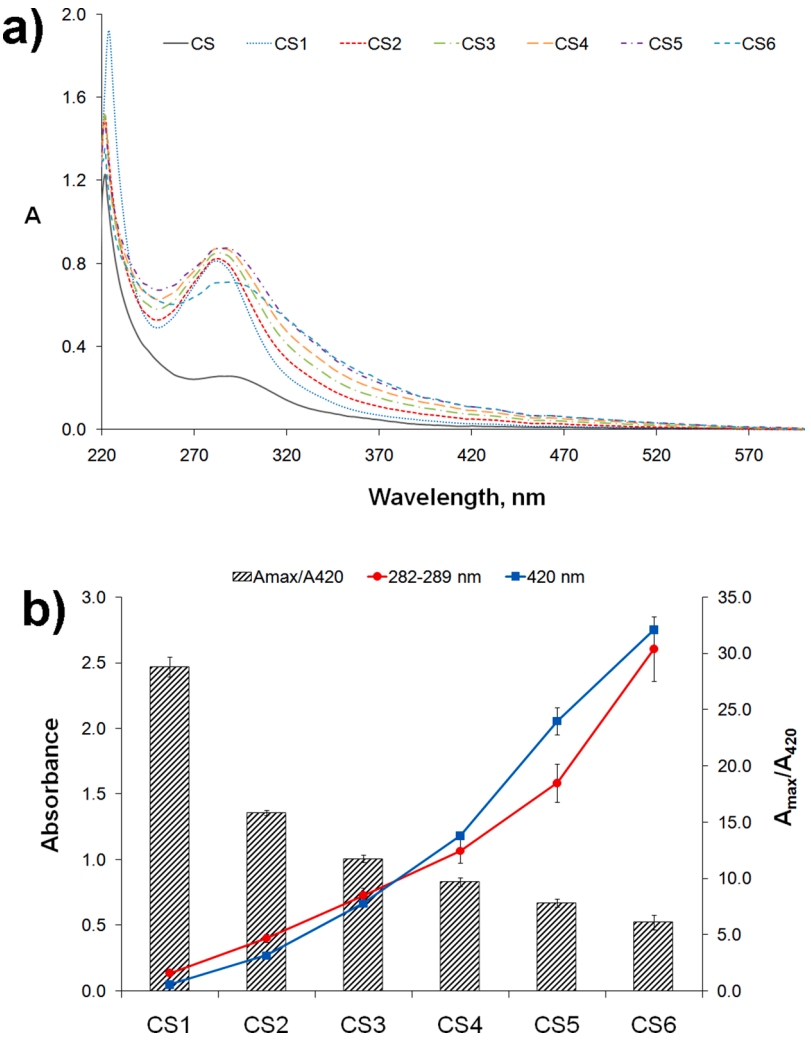

Fig. 1. UV-vis spectra of the neat and modified CS (a), and extent of the reaction (A_{max}/A_{420}) for CS1-CS6 (b).

increases with increasing concentration of chitosan (Fig. 3).

3.2. FTIR spectroscopy

FTIR spectra of CS acetate and CS5 range from 4000 to 400 cm^{-1} are presented in Fig. 4. In the spectrum of CS acetate characteristic bands at 3177 (O-H and N-H stretching), 2875 (C-H stretching), 1631 (C=O stretching vibrations, amide I), 1066 and 1019 (C-O stretching), 1152 and 891 (ν_{as}(C-O-C bridge) and C-H bending vibrations of glucopyranose ring), 652 cm^{-1} (δ(OCO) of acetic acid) were observed (Guimarães et al., 2020; Mauricio-Sánchez et al., 2018; Nikalaichuk et al., 2022; Tran et al., 2019). In addition, the spectrum of chitosan acetate is distinguished by two strong bands at 1536 and 1404 cm^{-1}. Some studies have reported that these bands are related to asymmetric and symmetric stretching vibrations of the carboxylate anion $–COO^-$ (Cervera et al., 2011; Mauricio-Sánchez et al., 2018). At the same time, the bands at 1536 and 1404 cm^{-1} often are assigned to the N-H bending vibrations (amide II) (El-Sayed et al., 2022; Guimarães et al., 2020; Tran et al., 2019) and the deformation of the -CH_2 groups respectively (Mauricio-Sánchez et al., 2018; Mucha et al., 2015; Yang et al., 2020).

The spectra of CS5 showed the increase in intensity of the C-O stretching vibration band at 1019 cm^{-1} and amide II band at 1536 cm^{-1}, and disappearance of the shoulder around 1710 cm^{-1} (attributed to carbonyl groups), which may indicate the changes in the structure of CS. The increase in intensity of the band at 1019 cm^{-1} (corresponding to the C-O stretching) after reaction of chitosan with glucose was also observed by authors (Gullón et al., 2016; Kosaraju et al., 2010). The authors (Arata Badano et al., 2019) have also reported about increase in intensity of the amide II band in FTIR spectrum of chitosan-lactose derivatives, synthesized by Maillard reaction.

3.3. NMR spectroscopy

^{1}H-NMR analysis was used to study structural changes in CS. The ^{1}H-NMR spectrum of chitosan and CS5 are shown in Fig. 5. The characteristic signals in the spectrum of CS were observed: the peak at δ 2.0 ppm belongs to methyl protons of N-acetyl glucosamine ($H_{N\text{-}COCH3}$), the peak at δ 3.0 ppm represents H-2 of glucosamine residues (H-2D), multiplet at δ 3.5-3.8 ppm - H-3-H-6 protons of the pyranose ring (Arata Badano et al., 2019; Kasaai, 2010; Tran et al., 2019). The protons of H-1 of N-acetyl glucosamine (H-1A) resonate at 4.5 ppm, while the protons of H-1 of glucosamine (H-1D), having a signal at 4.7-4.8 ppm (Arata Badano et al., 2019; Lee et al., 2014), overlaps with a strong signal at δ 4.7 ppm belonged to solvent (D_2O). The peak at 1.9 ppm is due to chemical shifts of protons in CH_3COOH, which is present in the neat CS and CS5 samples.

The degree of acetylation (DA) of CS acetate estimated by formula (7), proposed by the authors (Arata Badano et al., 2019; Kasaai, 2010), was 9.3%.

$$DA = [(1 / 3I_{N-COCH3} / I_{H-2}] \times 100 \quad (7)$$

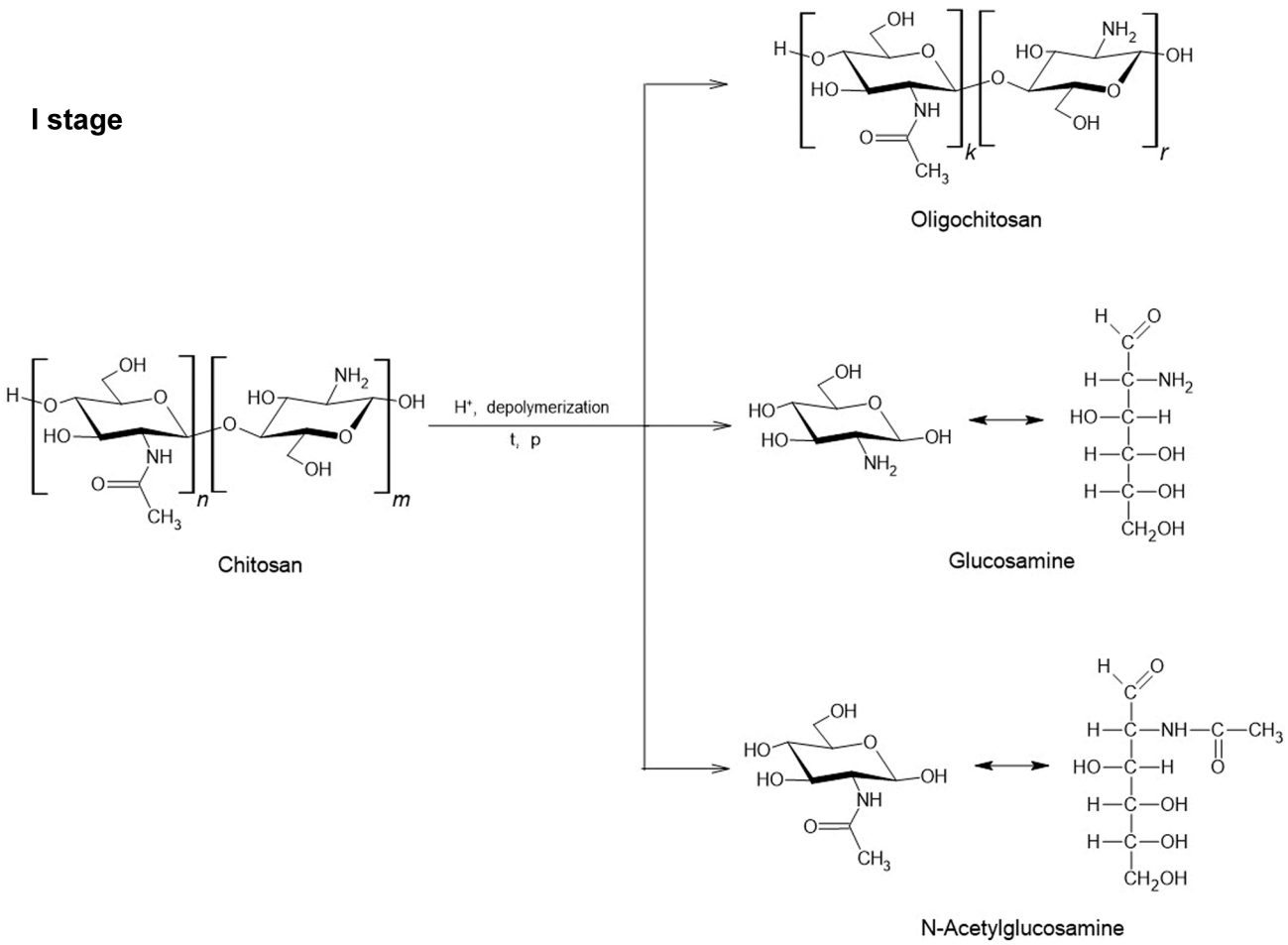

Fig. 2. Scheme of chitosan-based Maillard self-reaction (adapted and modified from Gullón et al. 2016, Tran et al. 2019).

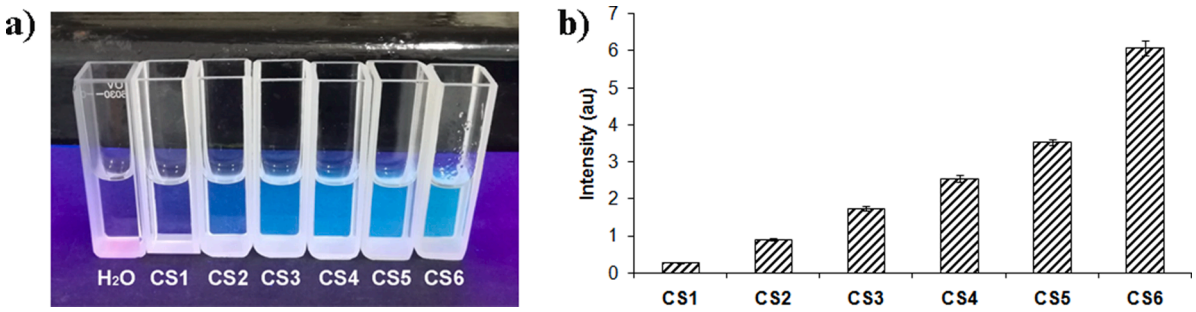

Fig. 3. The optical image under UV light (a) and fluorescence intensity (b) of the CS1-CS6 samples.

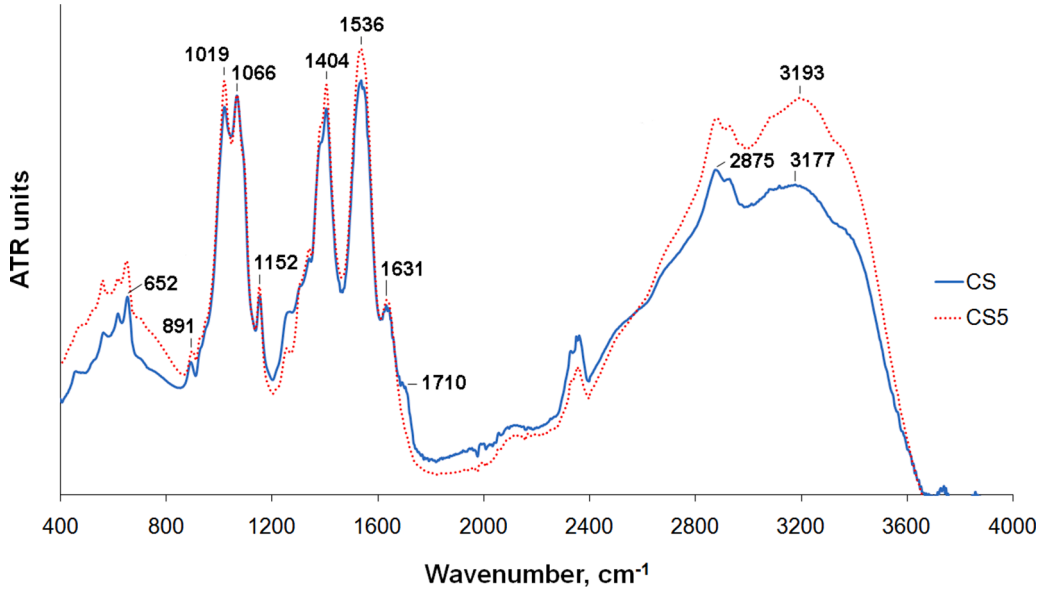

Fig. 4. FTIR spectra of the CS acetate and CS5 samples.

where $I_{N-COCH3}$ and I_{H-2} are integrals of methyl protons of N-acetyl glucosamine and H-2 proton of glucosamine, respectively.

After hydrothermal treatment the main structure of the polymer was preserved and the degree of acetylation did not significantly change: DA of CS5 was 10.7%. However, by comparing ^{1}H-NMR spectra some differences between CS and CS1-CS6 were found. A new signal at 1.5 ppm may relate to the proton of alkyl group (methine). A new signal at 2.07 ppm, corresponding to -CH_2 group linked to the -NH_2 group of CS, indicates a displacement of the -N=CH- linkage (Schiff base) toward –NH-CH_2– (Gullón et al., 2016). In the region around 4.5-4.6 ppm some signal also appeared that point to the N-substitution of the NH_2 groups of CS (Arata Badano et al., 2019; Gullón et al., 2016). Thus, the observed changes in the CS5 spectrum indicate an alteration in the structure of chitosan.

3.4. Thermogravimetric analysis

TG, DTG and DTA curves of CS acetate and CS1-CS6 samples are shown in Fig. 6. On the DTG curve of the CS acetate five consecutive weight loss steps were observed. The first stage was a weight loss about 11.6% below 115°C, attributed to physically adsorbed and/or weakly hydrogen-bonded water evaporation, while the second stage (from 115 to 196°C) was a weight loss about 11.8%, related to strongly hydrogen-bonded water release (Moussout et al., 2016; Zawadzki & Kaczmarek, 2010). The third stage in the range of 196-359°C was corresponded to depolymerization of chitosan and degradation of pyranose rings (Beyazit et al., 2020; C.-Eulalio et al., 2019; Corazzari et al., 2015; Zawadzki & Kaczmarek, 2010). During this stage 47.7% weight loss of CS was observed. The fourth stage (from 359 to 447°C) of weight loss (about 12.6%) could be attributed to the destruction of acetic acid (Corazzari et al., 2015). It should be noted that this peak was absent on the DTG curve of neat chitosan. And the fifth degradation step (from 447 to 600°C) was the thermo-oxidative process (C.-Eulalio et al., 2019; Zawadzki & Kaczmarek, 2010) and the destruction of chitosan residues (Moussout et al., 2016).

CS exhibited a broad endothermic peak at about 74°C on DTA curve, which was assigned to the loss of water (Beyazit et al., 2020; El-Hafian et al., 2010). The exothermic peaks centered at about 286 and 516°C were attributed to the thermal decomposition of the polymer and combustion of gaseous products formed during the decomposition of acetic acid, respectively (Corazzari et al., 2015).

After the hydrothermal treatment some changes in thermal behaviors of CS1-CS6 were established. The temperature at the maximum degradation rate of CS acetate and CS1-CS6 was 250-274°C (Table 1). The maximum degradation rate (peak depth) at this temperature decreased compared to CS acetate (from 2.6 %/min in the case of CS acetate to 1.9 %/min for CS5). Moreover, with increase in the CS concentration the weight loss, assigned to water evaporation (1st and 2nd stages), increased (Table 1), indicating a higher hydrophilicity of the CS1-CS5 samples compared to the initial CS acetate. In addition, the DTG curves of CS5 and CS6 samples showed that the peaks at final stage of thermal degradation are shifted and more pronounced than the same peaks of other samples, which confirms the structural differences between the samples. The thermal stability of CS1-CS6 samples did not

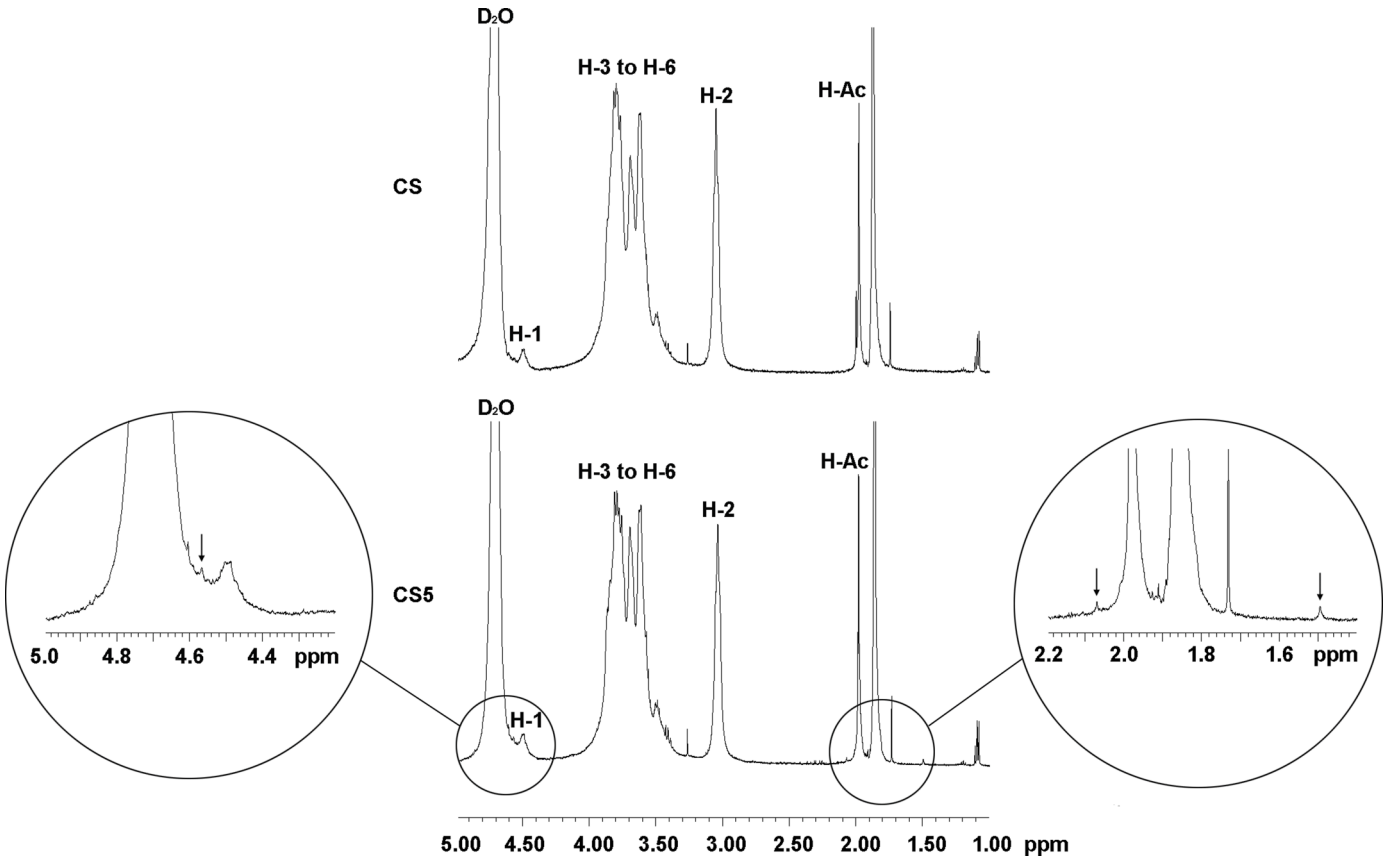

Fig. 5. NMR spectra of the CS and CS5 samples.

significantly change compared to CS acetate, indicating the invariance of the degree of deacetylation (Wanjun et al., 2005) of CS after hydrothermal treatment. This data was in good agreement with the NMR data mentioned above.

The yield of thermal degradation in oxygen/nitrogen atmosphere was very high, only 0-11% of char residue was found at 600°C (Table 1). Similar phenomena were also observed by (Zawadzki & Kaczmarek, 2010) for thermal degradation of chitosan in oxidized conditions.

3.5. XRD analysis

X-ray diffraction patterns of CS acetate and CS1-CS6 samples are illustrated in Fig. 7. CS acetate showed absence of any characteristic peak due to its amorphous nature. The similar effect was observed by authors (Cervera et al., 2011; Mauricio-Sánchez et al., 2018). It's could be due to the disruption of hydrogen bonds because of amino groups of glucosamine units of CS macromolecules in acetic acid are protonated (Fig. S2).

CS1-CS6 samples exhibited two diffraction peaks at around 9° and 12° (2θ), assigned to hydrated crystalline planes $(020)_h$ (hydrated polymorph of chitosan) and the anhydrous planes $(110)_a$, respectively (Facchinatto et al., 2020; Harish Prashanth, 2002). Moreover, in diffractogram of CS6 the crystalline peak of hydrated polymorph at approximately 18° (2θ) was observed (Nunthanid et al., 2001). This XRD data are in a good agreement with the TGA data obtained, showing the presence of water in the CS1-CS6 samples (Table 1). The halo diffraction patterns of CS1-CS6 at around 21-22° (2θ) indicated the amorphous state of the samples (Cervera et al., 2011; Nunthanid et al., 2001).

According to FTIR spectra, mentioned above, the broad peak at 3177 cm^{-1} (CS acetate), related to OH-stretching, became more narrow and shifted to higher frequency (3193 cm^{-1}) in the case of CS5, indicating the more ordered structure (Zhang et al., 2005). This data are in a good agreement with the XRD results, which demonstrated the increase in the ordered structure in the CS1 < CS2 < CS3 < CS4 < CS5 < CS6 series. It might be concluded that CS acetate was in amorphous state, while CS1-CS6 samples were in amorphous to partially crystalline state.

3.6. The viscosity-average molecular weight of MSRPs

One of the key factors in the efficiency of the Maillard reaction is the pH value: neutral or slightly alkaline pH is preferred (Gullón et al., 2016; Tessier et al., 2003; Zeng et al., 2007). However, chitosan is an acid-soluble polymer and has limited solubility in near-neutral media. At present work all chitosan solutions were prepared in 2% acetic acid. With an increase in the concentration of chitosan solution, the pH value increases from 3.5 (for CS1) to 4.0 (CS5), that can be explained by the cationic nature of chitosan macromolecules due to the presence of amino groups. During the dissolution of chitosan acetic acid is partially neutralized due to interaction with the amino groups of polymer. Therefore, as expected, with an increase in the concentration of chitosan solution a shift in the pH value occurs. After hydrothermal treatment the pH of the mixtures was 4.0. Chitosan macromolecules in an acidic medium under conditions of elevated temperature and pressure undergo hydrolysis of the glycosidic bond with the elimination of oligomers and monomers. Fig. 8 shows the viscosity-average molecular weight values for neat chitosan and CS1-CS5 samples.

Hydrothermal treatment of chitosan solutions leads to a significant decrease in the viscosity-average molecular weight of polymer compared to the initial value (Fig. 8). Such significant changes in the molecular weight of the polymer are primarily caused by the hydrolysis of the chitosan macromolecule in the acidic medium. The most significant decrease in M_v (up to 70%) of the CS1 solution was established. At the same time, with a tenfold increase in the concentration of chitosan a decrease in M_v does not exceed 33%. Thus, in dilute chitosan solutions

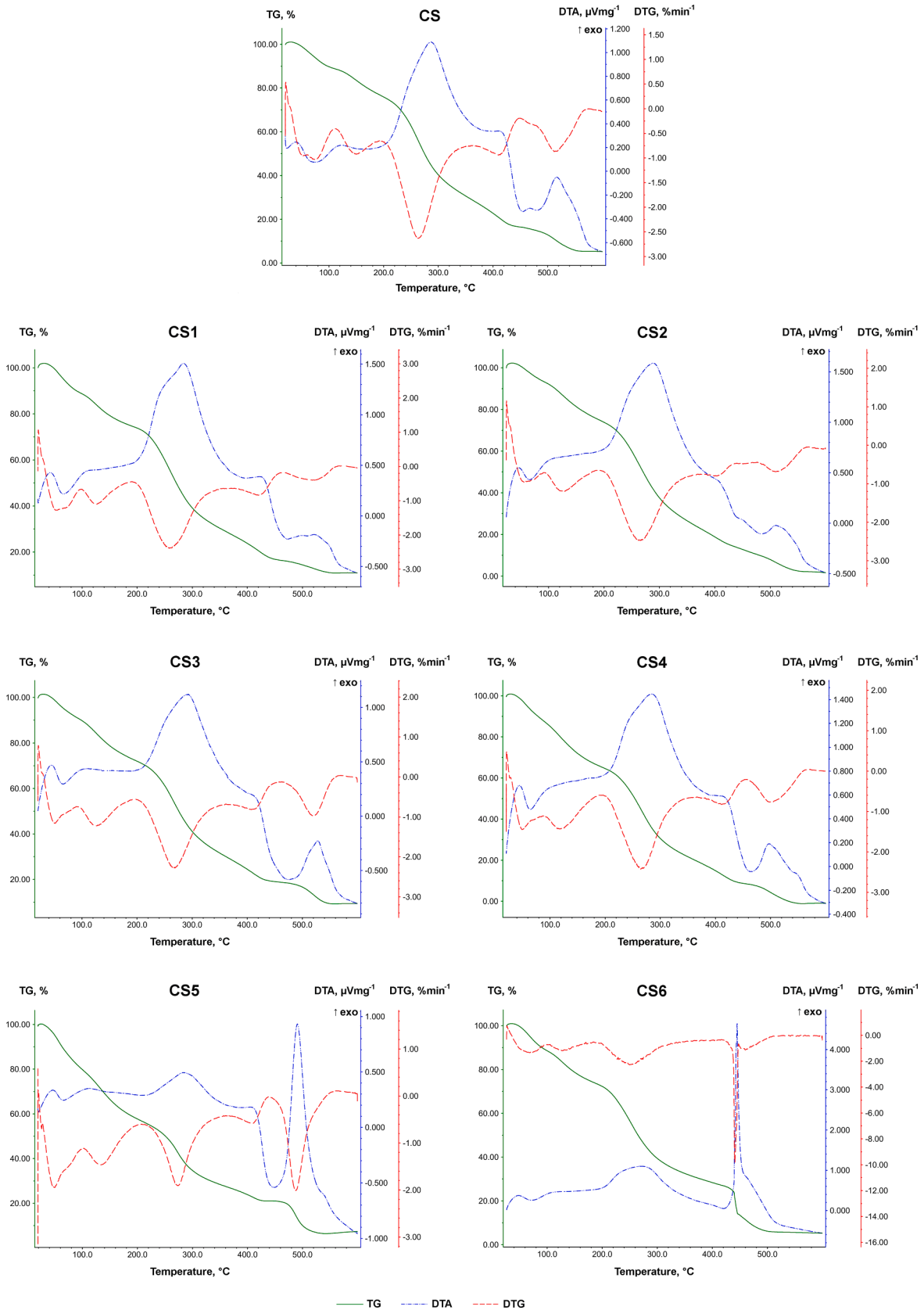

Fig. 6. TG, DTA and DTG curves obtained for thermal degradation of CS acetate and CS1-CS6.

Table 1
Thermal degradation steps of CS and CS1-CS6 samples.

Sample	Stage	Temperature range, °C	Temperature at maximum process rate, °C	Weight loss, %	Residual weight, %
CS acetate	1st	25-115	53 and 76	11.6	5.1
	2nd	115-196	150	11.8	
	3rd	196-359	263	47.7	
	4th	359-447	410	12.6	
	5th	447-600	512	11.2	
CS1	1st	25-100	54	11.2	10.7
	2nd	100-189	127	14.4	
	3rd	189-367	259	46.3	
	4th	367-462	420	12.0	
	5th	462-600	518	5.4	
CS2	1st	25-96	56	6.6	1.8
	2nd	96-195	127	18.7	
	3rd	195-371	262	50.7	
	4th	371-453	403	12.0	
	5th	453-600	510	10.2	
CS3	1st	25-95	51	9.3	9.2
	2nd	95-195	127	18.2	
	3rd	195-350	269	41.1	
	4th	350-464	408	13.1	
	5th	464-600	520	9.1	
CS4	1st	25-91	49	13.3	0
	2nd	91-195	119	21.3	
	3rd	195-347	265	43.0	
	4th	347-460	411	13.4	
	5th	460-600	503	9.0	
CS5	1st	25-102	50	20.2	7.9
	2nd	102-206	133	22.7	
	3rd	206-360	274	28.9	
	4th	360-441	411	6.6	
	5th	441-600	488	13.7	
CS6	1st	25-101	73	11.8	5.0
	2nd	101-193	127	15.2	
	3rd	193-420	250	46.3	
	4th	420-600	441	21.7	

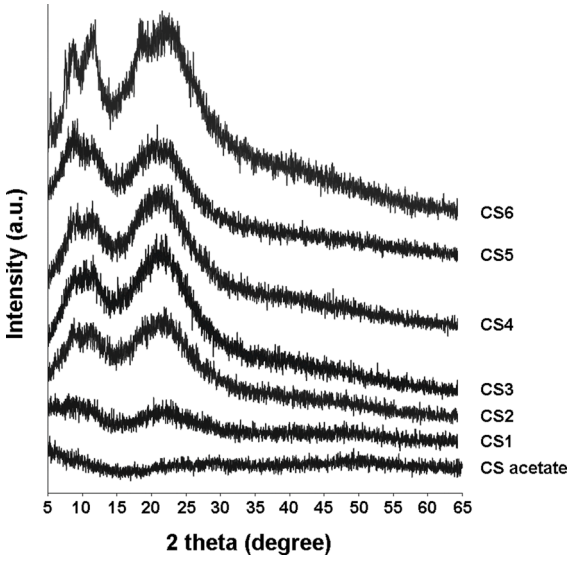

Fig. 7. X-ray diffraction patterns of the CS acetate and CS1-CS6 samples.

during hydrothermal treatment, hydrolytic degradation of the polymer (Fig. 2, I stage) was prevailed, which was accompanied by a significant decrease in the molecular weight of chitosan and viscosity of solutions. At the same time, destruction of the polymer was not so significant in solutions with a high concentration of chitosan.

The rate of the Maillard reaction strictly depends on the concentration of the reagents and the pH value, since pH is associated with the amount of free amino groups (Hafsa et al., 2021; Umemura & Kawai, 2007). Taking into account the hydrolysis of the polymer, the amount of eliminated oligo- and monosaccharide fragments of chitosan with reducing potential was significantly higher in solutions with a high concentration of chitosan (CS5) than in diluted ones (CS1). In addition, due to the neutralizing effect of chitosan, the number of non-protonated amino groups capable to form of Schiff bases increases with an increase in the concentration of polymer. Thus, during the hydrothermal treatment of chitosan solutions in acetic acid two processes occur simultaneously: hydrolytic degradation of the polymer and the Maillard reaction. Moreover, along with a large number of reactive non-protonated amino groups a greater number of reactive amino groups of the main chain in chitosan solutions with the high concentration ($\geq$ 20 mg/mL) in comparison with diluted solutions were observed. Both of these factors lead to a significant increase in the Maillard reaction rate. It is known that the chemistry of the Maillard reaction in an acidic medium is associated with the accumulation of high molecular weight melanoidins (Hafsa et al., 2021; Liu et al., 2020). Thus, the measured value of M_v for sample CS5 was ~ 45000 Da.

3.7. Antioxidant activity

The $ABTS^+$ radical-scavenging activity of CS and CS1-CS6 samples is shown in Fig. 9a and ranges from 1.42±0.09 to 7.10±0.47 μg AE/mg of the sample. The radical-scavenging activity of MSRPs was increased after MR: CS5 and CS6 samples showed the highest $ABTS^{\bullet+}$ scavenging activity. Comparative analysis of antiradical activity of CS1-CS6 samples showed its change in the CS1 < CS2 < CS3 < CS4 < CS5 ≈ CS6 series. Moreover, the antiradical activity of CS1-CS6 samples was 2-5 times higher in comparison with the activity of neat chitosan. Unfortunately, relevant researches are extremely little. The authors (Jung et al., 2014) have reported that prolonged heating of 2% solution of oligochitosan for 240 min led to increase in its antiradical activity only 2.2 times compared to neat oligomer.

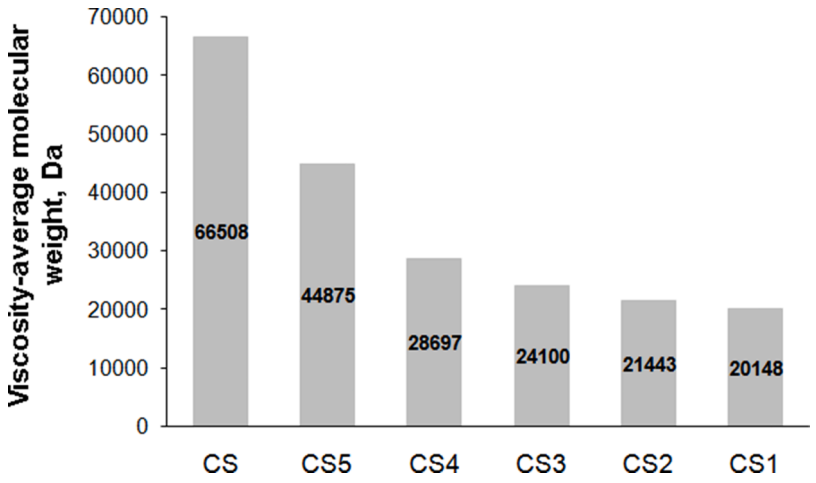

Fig. 8. The viscosity-average molecular weight of CS and CS1-CS5 samples.

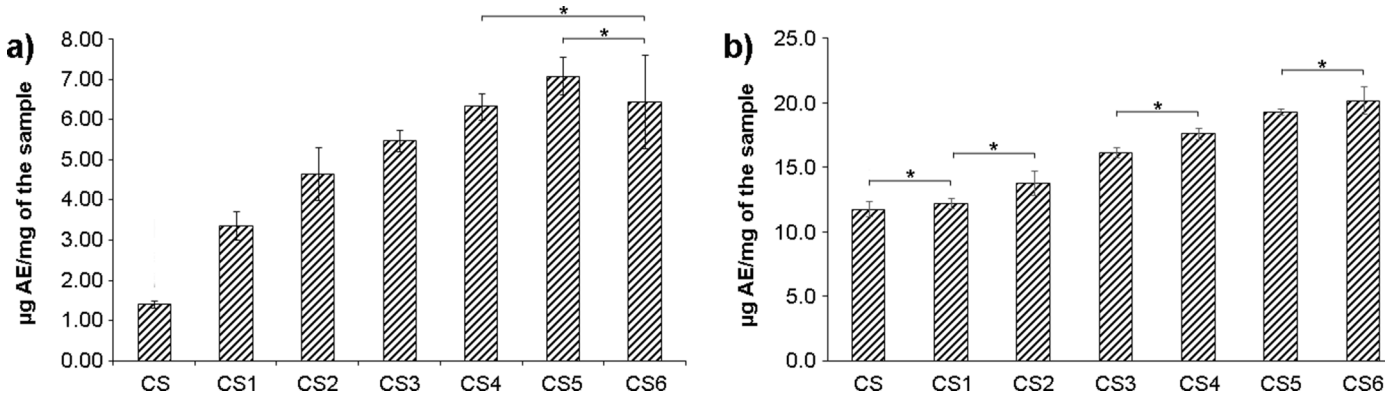

Fig. 9. Antiradical activity (a) and reducing power (b) of CS and CS1-CS6 samples
(The obtained data are statistically significant, $p < 0.05$. The data indicated by "asterisk" are statistically insignificant).

The common mechanism of radical-scavenging activity of chitosan and its derivatives is attributed to that amino and hydroxyl groups, which react with unstable free radicals to form stable macromolecule radicals (Sun et al., 2018; Tamer et al., 2016). The amino groups are partially consumed during MR of chitosan, and the antiradical activity of the derivatives depends on the structure of the embedded fragments (mono-, di- and oligosaccharides and/or proteins). Thus, in the case of glucose residues embedding, the number of hydroxyl groups capable of blocking radicals, increased, and the antioxidant properties improved (Sun et al., 2018). The similar effect for aminated derivative of chitosan due to the increase in the number of amino groups in the polymer structure was observed (Tamer et al., 2016). Thus, the increase in the radical-scavenging activity of chitosan-based Maillard self-reaction products may be associated with the increase in the number of hydroxyl and amino groups due to the conjugation of oligomeric and polymeric chains of chitosan with its monomeric fragments. However, the mechanism controlling the above observations clearly requires additional studies.

Reducing power assay has also been used to evaluate the stability of antioxidants to donate electrons. The reducing power of CS and CS1-CS6 samples is shown in Fig. 9b and ranges from 11.8±0.6 to 20.2±1.1 μg AE/mg of the sample. The reducing power of CS1-CS6 samples correlated well with increasing concentrations. Comparative analysis of reducing power of CS1-CS6 samples showed its change in the CS1 < CS2 < CS3 < CS4 < CS5 < CS6 series. It should be noted, that reducing power of CS1-CS6 samples was 1.1-1.7 times higher in comparison with the activity of neat chitosan. The reducing power of CS5 and CS6 was more pronounced.

It should be noted that the antioxidant activity data correlate with the browning and fluorescence intensity ones: the indicators increase in the CS1-CS2-CS3-CS4-CS5-CS6 series. Thus, the highest antioxidant activity of CS5 and CS6 samples can be explained by the higher concentration of chitosan-based products with an outstanding radical trapping effect and donating activity, formed at intermediate (reductones) and final (melanoidins) stages of the Maillard self-reaction.

The conjugates of chitosan with saccharides or proteins, obtained by MR, exhibited better *in vitro* antioxidant ability than neat chitosan in the wide range of assays: radical-scavenging activity, oxygen radical absorbing capacity, reducing power and chelating abilities (Hafsa et al., 2021). The some authors observed a threefold increase in antioxidant activity for MRPs obtained by heat treatment (100-110°C) of the mixtures of chitosan-galactose (Hafsa et al., 2019) and chitosan-xylan (Luo et al., 2013). It should be noted that MR products with such high antioxidant properties were obtained after 3 and 24 h respectively. The authors (Sun et al., 2018) also noted a dramatic increase in antioxidant activity for oligochitosan MRPs compared to neat oligochitosan during heat treatment (80°C in a reflux reactor for 12 h) of its mixtures with glucose and alanine. In this work, a heat-treated oligochitosan was used as a positive control, however, the treatment mode proposed by the authors does not provide a deep and complete MR in oligochitosan by themselves. At present work, the short-term hydrothermal treatment allows to modify the neat chitosan without any additives due to its higher conversion, which leads to the formation of MRPs with higher (up to 5 times) antioxidant activity.

3.8. Antibacterial activity

The assessment of antimicrobial activity of the CS samples after hydrothermal treatment was carried out according to the R value, characterized the bacterial killing efficiency:

$$R = \lg(C_{control} / C_{sample}) \quad (8)$$

where $C_{control}$ – cell concentration after incubation on control (CFU/mL); C_{sample} - cell concentration after incubation on the test sample (CFU/mL). Samples that presented a bacterial mortality higher than 99% (R > 2) were considered valid.

Table 2 shows the values of the R index for all the studied samples. As can be seen from the Table 2 the least antimicrobial effect of all studied samples was demonstrated by CS acetate. The maximum antimicrobial effect against *Staphylococcus* sp. BIM B-798G and *G. stearothermophilus* BIM B-140 was exerted by CS1 and CS2 samples, against *E. coli* BIM B-378 - by CS5. The strain *P. aeruginosa* BIM B-153 exhibited resistance to all studied samples.

The antimicrobial activity for most chitosan-based Maillard reaction products was reported (Hafsa et al., 2021), however, it did not always exceed the activity of the neat chitosan (Deng et al., 2020). The antibacterial effect of the neat chitosan is due to the interaction of NH_3^+ with various cellular structures - teichoic acids, lipopolysaccharides, membrane proteins, and, possibly, with nucleic acids, which confirms its effectiveness against both gram-positive and gram-negative bacteria (Li & Zhuang, 2020; Rabea et al., 2003). Several mechanisms of antimicrobial activity of chitosan derivatives obtained by the Maillard reaction were assumed. Inhibition of microbial growth by chitosan derivatives, as for chitosan, is also associated with the presence of amino groups that are not involved in the reaction, which disrupt the metabolism of the cell membrane (Mahae et al., 2011; Shaheen et al., 2016). Moreover, Maillard-type conjugates are also able to destabilize the bacterial cell membrane due to their excellent emulsifying properties (Kato, 2002). At the same time, antimicrobial activities of melanoidins are proposed to have conferred upon them by their chromophore fragments (Rufian--Henares & Morales, 2007). In addition, the antimicrobial activity of MRPs is mediated by chelation of Fe^{2+}, Zn^{2+}, Cu^{2+} and Mg^{2+} from the microbial membranes leading to its destabilization (Chung et al., 2005; Mondaca-Navarro et al., 2017). Furthermore, due to improved solubility, chitosan derivatives exhibited better antimicrobial activity at pH 6–7 while the chitosan solubility decreases at neutral pH by losing protonated cationic amino group formed at pH 5 (Hafsa et al., 2021).

It can be concluded that hydrothermal treatment of CS solutions leads to enhance their antimicrobial activity against gram-negative and gram-positive bacteria. *Geobacillus stearothermophilus* is a gram-positive, thermophilic highly heat-resistant spore-forming bacterium involved in the spoilage of canned foods, especially milk and dairy products (André et al., 2017; Lücking et al., 2013). CS1-CS5 samples exhibited antimicrobial activity against *G. stearothermophilus*, therefore, they are may be perspective as food preservatives.

Table 2
Antibacterial activity of CS and CS1-CS5 samples.

Bacteria strains	R CS acetate	CS1	CS2	CS3	CS4	CS5
Bacillus subtilis B-210	1.4	4.4	4.4	4.4	4.4	4.4
Staphylococcus sp. B-798G	2.2	4.6	4.9	3.6	3.8	3.6
Escherihia coli B-378	2.1	1.7	1.6	1.6	1.8	3.0
Pseudomonas aeruginosa B-153	N/A	N/A	N/A	N/A	N/A	N/A
Geobacillus stearothermophilus B-140	3.2	4.8	5.0	3.8	3.9	3.8

N/A – No antibacterial activity was found

4. Conclusion

In this study, it was reported that modification of chitosan was carried out by Maillard self-reaction without any additives via short-term hydrothermal treatment. The formation of chitosan derivatives was confirmed by UV–Vis, FTIR, ^{1}H NMR spectroscopy, TG and XRD analyses. The antioxidant assays showed the excellent enhancement (up to 5 times) in the antioxidant activity of chitosan-based Maillard reaction products. Furthermore, the same effect was observed for antimicrobial activity of modified chitosan: the derivatives exhibited enhanced antimicrobial action against gram-negative and gram-positive bacteria including thermophilic highly heat-resistant *G. stearothermophilus*. Therefore, they may be regarded as promising food preservatives. These results support the hypothesis that the modification of chitosan via hydrothermal treatment leads to enhancing the antioxidant and antimicrobial activities of polysaccharide. This approach is an eco-friendly, simple and inexpensive way to improve the functional properties of the polymer.

Declaration of Competing Interest

The authors declare that they have no conflict of interest.

Data availability

Data will be made available on request.

Acknowledgements

This study was financially supported by Belarusian Republican Foundation for Fundamental Research (grant no. X22KI-011) and the National Natural Science Foundation of China (3211101620).

Supplementary materials

Supplementary material associated with this article can be found, in the online version, at doi:10.1016/j.carpta.2022.100257.

References

Affes, S., Nasri, R., Li, S., Thami, T., Van Der Lee, A., Nasri, M., & Maalej, H. (2021). Effect of glucose-induced Maillard reaction on physical, structural and antioxidant properties of chitosan derivatives-based films. *Carbohydrate Polymers, 255*, Article 117341. https://doi.org/10.1016/j.carbpol.2020.117341

Alexandrova, V. A., Domnina, N. S., & Snigireva, G. P. (2016). Antimutagenic systems based on chitosan conjugates with plant antioxidants. *Applied Biochemistry and Microbiology, 52*(5), 491–495. https://doi.org/10.1134/S0003683816050033

André, S., Vallaeys, T., & Planchon, S. (2017). Spore-forming bacteria responsible for food spoilage. *Research in Microbiology, 168*(4), 379–387. https://doi.org/10.1016/j.resmic.2016.10.003

Arata Badano, J., Vanden Braber, N., Rossi, Y., Díaz Vergara, L., Bohl, L., Porporatto, C., Dario Falcone, R., & Montenegro, M. (2019). Physicochemical, *in vitro* antioxidant and cytotoxic properties of water-soluble chitosan-lactose derivatives. *Carbohydrate Polymers, 224*, Article 115158. https://doi.org/10.1016/j.carbpol.2019.115158

Bakshi, P. S., Selvakumar, D., Kadirvelu, K., & Kumar, N. S. (2020). Chitosan as an environment friendly biomaterial – a review on recent modifications and applications. *International Journal of Biological Macromolecules, 150*, 1072–1083. https://doi.org/10.1016/j.ijbiomac.2019.10.113

Beyazit, N., Çakran, H. S., Cabir, A., Akışcan, Y., & Demetgül, C. (2020). Synthesis, characterization and antioxidant activity of chitosan Schiff base derivatives bearing (−)-gossypol. *Carbohydrate Polymers, 240*, Article 116333. https://doi.org/10.1016/j.carbpol.2020.116333

C.-Eulalio, H. Y., B.-Rodrigues, J. F., O.-Santos, K., Peniche, C., & V.-LiaFook, M. (2019). Characterization and thermal properties of chitosan films prepared with different acid solvents. *Revista Cubana de Química, 31*(3), 309–323.

Cervera, M. F., Heinämäki, J., de la Paz, N., López, O., Maunu, S. L., Virtanen, T., Hatanpää, T., Antikainen, O., Nogueira, A., Fundora, J., & Yliruusi, J. (2011). Effects of spray drying on physicochemical properties of chitosan acid salts. *AAPS PharmSciTech, 12*(2), 637–649. https://doi.org/10.1208/s12249-011-9620-3

Chang, H. L., Chen, Y. C., & Tan, F. J. (2011). Antioxidative properties of a chitosan–glucose Maillard reaction product and its effect on pork qualities during refrigerated storage. *Food Chemistry, 124*(2), 589–595. https://doi.org/10.1016/j.foodchem.2010.06.080

Chung, Y. C., Kuo, C. L., & Chen, C. C. (2005). Preparation and important functional properties of water-soluble chitosan produced through Maillard reaction. *Bioresource Technology, 96*(13), 1473–1482. https://doi.org/10.1016/j.biortech.2004.12.001

Corazzari, I., Nisticò, R., Turci, F., Faga, M. G., Franzoso, F., Tabasso, S., & Magnacca, G. (2015). Advanced physico-chemical characterization of chitosan by means of TGA coupled on-line with FTIR and GCMS: Thermal degradation and water adsorption capacity. *Polymer Degradation and Stability, 112*, 1–9. https://doi.org/10.1016/j.polymdegradstab.2014.12.006

Deng, W., Luo, J., & Yan, X. (2020). Maillard reaction between chitosan and xylan in ionic liquids. *Ferroelectrics, 562*(1), 39–45. https://doi.org/10.1080/00150193.2020.1760582

El-Hafian, E. A., Elgannoudi, E. S., Mainal, A., & Yahaya, A. (2010). Characterization of chitosan in acetic acid: Rheological and thermal studies. *Turkish Journal of Chemistry, 34*, 47–56. https://doi.org/10.3906/kim-0901-38

El-Sayed, N. S., Hashem, A. H., & Kamel, S. (2022). Preparation and characterization of Gum Arabic Schiff's bases based on 9-aminoacridine with *in vitro* evaluation of their antimicrobial and antitumor potentiality. *Carbohydrate Polymers, 277*, Article 118823. https://doi.org/10.1016/j.carbpol.2021.118823

Facchinatto, W. M., Santos, D. M., dos, Fiamingo, A., Bernardes-Filho, R., Campana-Filho, S. P., de Azevedo, E. R., & Colnago, L. A. (2020). Evaluation of chitosan crystallinity: A high-resolution solid-state NMR spectroscopy approach. *Carbohydrate Polymers, 250*, Article 116891. https://doi.org/10.1016/j.carbpol.2020.116891

Guimarães, M. F., Pighinelli, L., Paz, R. L., Kmiec, M., Zehetmeyer, G., Becker, C. M., Escobar, C. F., & Dos Santos, L. A. (2020). Chemical and physical properties of nanocrystalline chitosan by the method: Modified nanochitosan complex and process of obtaining modified nanochitosan. *Carbohydrate Research, 493*, Article 108035. https://doi.org/10.1016/j.carres.2020.108035

Gullón, B., Montenegro, M. I., Ruiz-Matute, A. I., Cardelle-Cobas, A., Corzo, N., & Pintado, M. E. (2016). Synthesis, optimization and structural characterization of a chitosan–glucose derivative obtained by the Maillard reaction. *Carbohydrate Polymers, 137*, 382–389. https://doi.org/10.1016/j.carbpol.2015.10.075

Hafsa, J., Smach, M. A., Mrid, R. Ben, Sobeh, M., Majdoub, H., & Yasri, A. (2021). Functional properties of chitosan derivatives obtained through Maillard reaction: A novel promising food preservative. *Food Chemistry, 349*, Article 129072. https://doi.org/10.1016/j.foodchem.2021.129072

Hafsa, J., Smach, M. A., Sobeh, M., Majdoub, H., & Yasri, A. (2019). Antioxidant activity improvement of apples juice supplemented with chitosan-galactose Maillard reaction products. *Molecules, 24*(24), 4557. https://doi.org/10.3390/molecules24244557

Harish Prashanth, K. (2002). Solid state structure of chitosan prepared under different N-deacetylating conditions. *Carbohydrate Polymers, 50*(1), 27–33. https://doi.org/10.1016/S0144-8617(01)00371-X

Jung, W. K., Park, P. J., Ahn, C. B., & Je, J. Y. (2014). Preparation and antioxidant potential of Maillard reaction products from (MRPs) chitooligomer. *Food Chemistry, 145*, 173–178. https://doi.org/10.1016/j.foodchem.2013.08.042

Kaewtathip, T., Wattana-Amorn, P., Boonsupthip, W., Lorjaroenphon, Y., & Klinkesorn, U. (2022). Maillard reaction products-based encapsulant system formed between chitosan and corn syrup solids: Influence of solution pH on formation kinetic and antioxidant activity. *Food Chemistry, 393*, Article 133329. https://doi.org/10.1016/j.foodchem.2022.133329

Kanatt, S. R., Chander, R., & Sharma, A. (2008). Chitosan glucose complex – a novel food preservative. *Food Chemistry, 106*(2), 521–528. https://doi.org/10.1016/j.foodchem.2007.06.036

Kasaai, M. R. (2007). Calculation of Mark–Houwink–Sakurada (MHS) equation viscometric constants for chitosan in any solvent–temperature system using experimental reported viscometric constants data. *Carbohydrate Polymers, 68*(3), 477–488. https://doi.org/10.1016/j.carbpol.2006.11.006

Kasaai, M. R. (2010). Determination of the degree of N-acetylation for chitin and chitosan by various NMR spectroscopy techniques: A review. *Carbohydrate Polymers, 79*(4), 801–810. https://doi.org/10.1016/j.carbpol.2009.10.051

Kato, A. (2002). Industrial applications of Maillard-type protein-polysaccharide conjugates. *Food Science and Technology Research, 8*(3), 193–199. https://doi.org/10.3136/fstr.8.193

Kosaraju, S. L., Weerakkody, R., & Augustin, M. A. (2010). Chitosan−glucose conjugates: Influence of extent of Maillard reaction on antioxidant properties. *Journal of Agricultural and Food Chemistry, 58*(23), 12449–12455. https://doi.org/10.1021/jf103484z

Lee, D. S., Woo, J. Y., Ahn, C. B., & Je, J. Y. (2014). Chitosan–hydroxycinnamic acid conjugates: Preparation, antioxidant and antimicrobial activity. *Food Chemistry, 148*, 97–104. https://doi.org/10.1016/j.foodchem.2013.10.019

Li, D., Xie, Y., Na, X., Li, Y., Dai, C., Li, Y., & Tan, M. (2019). Insights into melanoidin conversion into fluorescent nanoparticles in the Maillard reaction. *Food & Function, 10*(7), 4414–4422. https://doi.org/10.1039/C9FO00383E

Li, J., & Zhuang, S. (2020). Antibacterial activity of chitosan and its derivatives and their interaction mechanism with bacteria: Current state and perspectives. *European Polymer Journal, 138*, Article 109984. https://doi.org/10.1016/j.eurpolymj.2020.109984

Liu, X., Xia, B., Hu, L., Ni, Z., Thakur, K., & Wei, Z. (2020). Maillard conjugates and their potential in food and nutritional industries: A review. *Food Frontiers, 1*(4), 382–397. https://doi.org/10.1002/fft2.43

Lücking, G., Stoeckel, M., Atamer, Z., Hinrichs, J., & Ehling-Schulz, M. (2013). Characterization of aerobic spore-forming bacteria associated with industrial dairy processing environments and product spoilage. *International Journal of Food Microbiology, 166*(2), 270–279. https://doi.org/10.1016/j.ijfoodmicro.2013.07.004

Luo, Y., Ling, Y., Wang, X., Han, Y., Zeng, X., & Sun, R. (2013). Maillard reaction products from chitosan–xylan ionic liquid solution. *Carbohydrate Polymers, 98*(1), 835–841. https://doi.org/10.1016/j.carbpol.2013.06.023

Mahae, N., Chalat, C., & Muhamud, P. (2011). Antioxidant and antimicrobial properties of chitosan-sugar complex. *International Food Research Journal, 18*(4), 1543–1551.

Matiacevich, S. B., Santagapita, P. R., & Buera, M. P. (2005). Fluorescence from the Maillard reaction and its potential applications in food science. *Critical Reviews in Food Science and Nutrition, 45*(6), 483–495. https://doi.org/10.1080/10408390591034472

Mauricio-Sánchez, R. A., Salazar, R., Luna-Bárcenas, J. G., & Mendoza-Galván, A. (2018). FTIR spectroscopy studies on the spontaneous neutralization of chitosan acetate films by moisture conditioning. *Vibrational Spectroscopy, 94*, 1–6. https://doi.org/10.1016/j.vibspec.2017.10.005

Mondaca-Navarro, B. A., Ávila-Villa, L. A., González-Córdova, A. F., López-Cervantes, J., Sánchez-Machado, D. I., Campas-Baypoli, O. N., & Rodríguez-Ramírez, R. (2017). Antioxidant and chelating capacity of Maillard reaction products in amino acid-sugar model systems: applications for food processing. *Journal of the Science of Food and Agriculture, 97*(11), 3522–3529. https://doi.org/10.1002/jsfa.8206

Morales, F. J., & Jiménez-Pérez, S. (2001). Free radical scavenging capacity of Maillard reaction products as related to colour and fluorescence. *Food Chemistry, 72*(1), 119–125. https://doi.org/10.1016/S0308-8146(00)00239-9

Moussout, H., Ahlafi, H., Aazza, M., & Bourakhouadar, M. (2016). Kinetics and mechanism of the thermal degradation of biopolymers chitin and chitosan using thermogravimetric analysis. *Polymer Degradation and Stability, 130*, 1–9. https://doi.org/10.1016/j.polymdegradstab.2016.05.016

Mucha, M., Ksiazek, S., & Kaczmarek, H. (2015). Activation energy of copper-induced thermal degradation of chitosan acetate functional groups. *Journal of Polymer Engineering, 35*(3), 231–239. https://doi.org/10.1515/polyeng-2014-0157

Muzzarelli, R., Mehtedi, M., & Mattioli-Belmonte, M. (2014). Emerging biomedical applications of nano-chitins and nano-chitosans obtained via advanced eco-friendly technologies from marine resources. *Marine Drugs, 12*(11), 5468–5502. https://doi.org/10.3390/md12115468

Nikalaichuk, V., Hileuskaya, K., Kraskouski, A., Kulikouskaya, V., Nedved, H., Kalatskaja, J., Rybinskaya, E., Herasimovich, K., Laman, N., & Agabekov, V. (2022). Chitosan-hydroxycinnamic acid conjugates: Synthesis, photostability and phytotoxicity to seed germination of barley. *Journal of Applied Polymer Science, 139*(14), 51884. https://doi.org/10.1002/app.51884

Nooshkam, M., Falah, F., Zareie, Z., Tabatabaei Yazdi, F., Shahidi, F., & Mortazavi, S. A. (2019). Antioxidant potential and antimicrobial activity of chitosan–inulin conjugates obtained through the Maillard reaction. *Food Science and Biotechnology, 28*(6), 1861–1869. https://doi.org/10.1007/s10068-019-00635-3

Nunthanid, J., Puttipipatkhachorn, S., Yamamoto, K., & Peck, G. E. (2001). Physical properties and molecular behavior of chitosan films. *Drug Development and Industrial Pharmacy, 27*(2), 143–157. https://doi.org/10.1081/DDC-100000481

Quinto, E. J., Caro, I., Villalobos-Delgado, L. H., Mateo, J., De-Mateo-Silleras, B., & Redondo-Del-Río, M. P. (2019). Food safety through natural antimicrobials. *Antibiotics, 8*(4), 208. https://doi.org/10.3390/antibiotics8040208

Rabea, E. I., Badawy, M. E. T., Stevens, C. V., Smagghe, G., & Steurbaut, W. (2003). Chitosan as antimicrobial agent: Applications and mode of action. *Biomacromolecules, 4*(6), 1457–1465. https://doi.org/10.1021/bm034130m

Rao, M. S., Chawla, S. P., Chander, R., & Sharma, A. (2011). Antioxidant potential of Maillard reaction products formed by irradiation of chitosan–glucose solution. *Carbohydrate Polymers, 83*(2), 714–719. https://doi.org/10.1016/j.carbpol.2010.08.045

Re, R., Pellegrini, N., Proteggente, A., Pannala, A., Yang, M., & Rice-Evans, C. (1999). Antioxidant activity applying an improved ABTS radical cation decolorization assay. *Free Radical Biology and Medicine, 26*(9-10), 1231–1237. https://doi.org/10.1016/S0891-5849(98)00315-3

Rufian-Henares, J. A., & Morales, F. J. (2007). Antimicrobial activity of melanoidins. *Journal of Food Quality, 30*(2), 160–168. https://doi.org/10.1111/j.1745-4557.2007.00112.x

Shaheen, M., Shaaban, H., Hussein, A., Ahmed, M., El-Massry, K., & El-Ghorab, A. (2016). Evaluation of chitosan/fructose model as an antioxidant and antimicrobial agent for shelf life extension of beef meat during freezing. *Polish Journal of Food and Nutrition Sciences, 66*(4), 295–302. https://doi.org/10.1515/pjfns-2015-0054

Sun, T., Qin, Y., Xie, J., Xue, B., Zhu, Y., Wu, J., Bian, X., & Li, X. (2018). Antioxidant activity of oligochitosan Maillard reaction products using oligochitosan as the amino or carbonyl groups donors. *International Journal of Food Properties, 21*(1), 1964–1971. https://doi.org/10.1080/10942912.2018.1493605

Tamer, T., Valachová, K., Mohyeldin, M., & Soltes, L. (2016). Free radical scavenger activity of chitosan and its aminated derivative. *Journal of Applied Pharmaceutical Science, 6*(04), 195–201. https://doi.org/10.7324/JAPS.2016.60428

Tessier, F. J., Monnier, V. M., Sayre, L. M., & Kornfield, J. A. (2003). Triosidines: novel Maillard reaction products and cross-links from the reaction of triose sugars with lysine and arginine residues. *Biochemical Journal, 369*(3), 705–719. https://doi.org/10.1042/bj20020668

Tran, T. N., Doan, C. T., Nguyen, V. B., Nguyen, A. D., & Wang, S. L. (2019). Anti-oxidant and anti-diabetes potential of water-soluble chitosan–glucose derivatives produced by Maillard reaction. *Polymers, 11*(10), 1714. https://doi.org/10.3390/polym11101714

Umemura, K., & Kawai, S. (2007). Modification of chitosan by the Maillard reaction using cellulose model compounds. *Carbohydrate Polymers, 68*(2), 242–248. https://doi.org/10.1016/j.carbpol.2006.12.014

Varlamov, V. P., Il'ina, A. V., Shagdarova, B. T., Lunkov, A. P., & Mysyakina, I. S. (2020). Chitin/chitosan and its derivatives: Fundamental problems and practical

approaches. *Biochemistry (Moscow), 85*(S1), 154–176. https://doi.org/10.1134/S0006297920140084

Verlee, A., Mincke, S., & Stevens, C. V. (2017). Recent developments in antibacterial and antifungal chitosan and its derivatives. *Carbohydrate Polymers, 164*, 268–283. https://doi.org/10.1016/j.carbpol.2017.02.001

Wanjun, T., Cunxin, W., & Donghua, C. (2005). Kinetic studies on the pyrolysis of chitin and chitosan. *Polymer Degradation and Stability, 87*(3), 389–394. https://doi.org/10.1016/j.polymdegradstab.2004.08.006

Ways, T. M. M., Lau, W., & Khutoryanskiy, V. (2018). Chitosan and its derivatives for application in mucoadhesive drug delivery systems. *Polymers, 10*(3), 267. https://doi.org/10.3390/polym10030267

Yang, H., Zhang, Y., Zhou, F., Guo, J., Tang, J., Han, Y., Li, Z., & Fu, C. (2020). Preparation, bioactivities and applications in food industry of chitosan-based maillard products: A review. *Molecules, 26*(1), 166. https://doi.org/10.3390/molecules26010166

Zawadzki, J., & Kaczmarek, H. (2010). Thermal treatment of chitosan in various conditions. *Carbohydrate Polymers, 80*(2), 394–400. https://doi.org/10.1016/j.carbpol.2009.11.037

Zeng, L., Qin, C., Chi, W., Wang, L., Ku, Z., & Li, W. (2007). Browning of chitooligomers and their optimum preservation. *Carbohydrate Polymers, 67*(4), 551–558. https://doi.org/10.1016/j.carbpol.2006.06.029

Zhang, Y., Xue, C., Xue, Y., Gao, R., & Zhang, X. (2005). Determination of the degree of deacetylation of chitin and chitosan by X-ray powder diffraction. *Carbohydrate Research, 340*(11), 1914–1917. https://doi.org/10.1016/j.carres.2005.05.005